



Selective palladium nanoparticles-catalyzed hydrogenolysis of industrially targeted epoxides in water



Marion Duval^{a,b}, Victor Deboos^a, Agnès Hallonet^b, Gilles Sagorin^b, Audrey Denicourt-Nowicki^{a,*}, Alain Roucoux^{a,*}

^a Univ Rennes, Ecole Nationale Supérieure de Chimie de Rennes, CNRS, ISCR – UMR6226, F- 35000 Rennes, France

^b Dérivés Résiniques et Terpéniques, 1220 Route André Dupuy, 40260 Castets, France

ARTICLE INFO

Article history:

Received 17 December 2020

Revised 18 February 2021

Accepted 23 February 2021

Available online 04 March 2021

Keywords:

Palladium

Nanoparticles

Epoxides

Hydrogenolysis

Water

ABSTRACT

Palladium nanoparticles, with core sizes of *ca.* 2.5 nm, were easily synthesized by chemical reduction of Na₂PdCl₄ in the presence of hydroxyethylammonium salts and proved to be efficient for the selective hydrogenolysis of various aromatic, alkylphenyl, aliphatic epoxides in water as green solvent. Capping agents of the metal species were screened to define the most suitable micellar nanoreactors on two target substrates of industrial interest, epoxystyrene and 7,8-epoxy-2-methoxy-2,6-dimethyloctane. In our conditions, the hydrogenolysis of epoxystyrene proved to be pH-dependent, producing either the diol under acidic conditions, or the sweet-smelling 2-phenylethanol in the presence of a base. Promisingly, 7,8-epoxy-2-methoxy-2,6-dimethyloctane was completely and selectively hydrogenated into Florsantol[®], a sandalwood odorant at a multigram scale (40 g and up to 175g). A general mechanism for the palladium nanoparticles-catalyzed hydrogenolysis of terminal epoxides was proposed according to steric and electronic properties and finely corroborated with deuterium labelling experiments.

© 2021 Elsevier Inc. All rights reserved.

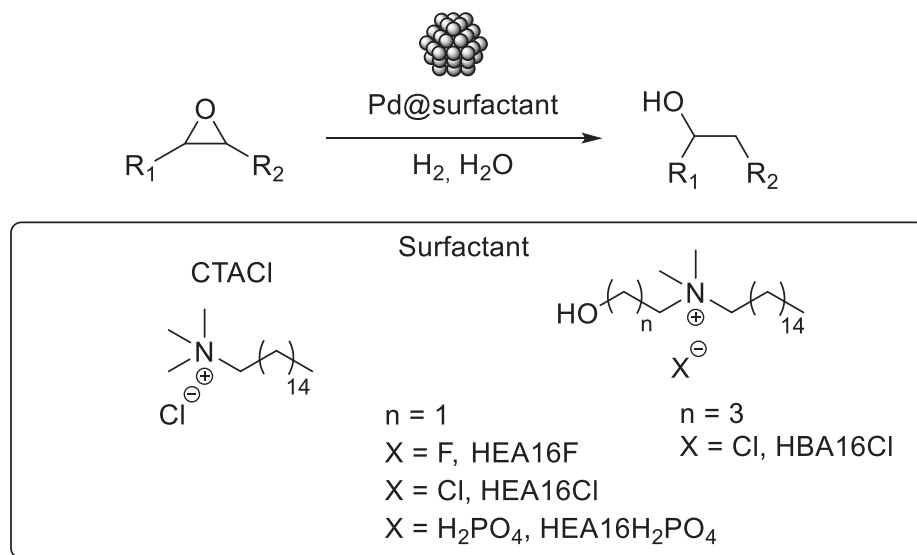
1. Introduction

The reductive ring-opening of oxiranes constitutes a paramount organic transformation [1,2], giving access to alcohols as relevant synthons for fine chemistry and fragrance industry. Historically, this reduction used to be performed with metal hydrides, which afford a mixture of alcohols and generate large amounts of polluting waste [3,4]. In the drive towards chemical processes of low environmental footprint and economically viable cost, the opening of epoxides through metal-catalyzed hydrogenolysis using molecular dihydrogen as a clean reducing agent has been extensively studied. The design of active and selective catalysts, as well as the use of green solvents and atom-saving reagents, remains of great interest for industrial applications [5,6]. In that context, molecular complexes have been designed to control the opening of epoxides to selectively provide either the primary [7,8] or the secondary [9,10] alcohol. Heterogeneous catalysts have also been used, such as modified Raney nickel at the early stage as well as palladium on charcoal with a higher occurrence [2,11,12], with good results for the reduction of terminal epoxides, but

substrate-dependent selectivity [13]. Recently, nanocatalysts proved to be pertinent tools, affording relevant catalytic performances owing to their unique surface reactivity [14,15]. Supported metal nanoparticles have been applied for this reaction in organic media, such as a TiO₂-supported Pt photocatalyst [16], Pd particles encapsulated in polyurea [17] or deposited on iron oxide [18], as well as Pd nanospecies loaded on cucurbit[6]uril in water [19]. In place of organic solvents, water has appeared as a cheap and green reaction media [20], potentially affording unique kinetics and selectivity [21]. To our knowledge, only one example of Pd nanospecies in water has been reported [22], providing primary alcohols for the hydrogenolysis of benzylic epoxides solely. Herein, we describe the use of hydroxylated ammonium-capped Pd nanoparticles in pure water for the selective hydrogenation of various aromatic, alkylphenyl or aliphatic epoxides (Scheme 1). Moreover, the reductive ring-opening of two target epoxides has been optimized, leading to added-value alcohols for fragrance industry. 2-Phenylethanol, obtained from styrene oxide, is a key ingredient of perfumes or soaps owing to its faint but lasting odor of rose petals, as well as in antiseptic creams and deodorants due to its bacteriostatic and antifungal properties [23]. The production of the industrially targeted Florsantol[®], a sought-after sandalwood odorant also known as Osyrol [24], was investigated via this biphasic substrate-water process on a multigram scale in collaboration

* Corresponding authors.

E-mail addresses: audrey.denicourt@ensc-rennes.fr (A. Denicourt-Nowicki), alain.roucoux@ensc-rennes.fr (A. Roucoux).



Scheme 1. Selective Pd(0) nanoparticles-catalyzed hydrogenolysis of epoxides.

with the “Dérivés Résiniques et Terpéniques” (DRT) company (Castets, France).

2. Materials and methods

2.1. Starting materials

Sodium tetrachloropalladate hydrate ($\text{Na}_2\text{PdCl}_4 \cdot 6\text{H}_2\text{O}$) was purchased from Strem Chemicals, and sodium borohydride (NaBH_4) from Acros Organics. Pd/C (5 wt%), polyvinylpyrrolidone (PVP), cetyltrimethyl ammonium chloride (CTACl), aqueous solution (30 wt%) of hexadecyl(2-hydroxyethyl)dimethylammonium dihydrogen phosphate ($\text{HEA16H}_2\text{PO}_4$) were obtained from Aldrich and were used without further purification. Other *N,N*-dimethyl-*N*-cetyl-*N*-(2-hydroxyalkyl)ammonium salts used were synthesized according to a procedure already reported in the literature [25–27]. Epoxystyrene, 2-benzylloxirane, 1,2-epoxybutane and 1,2-epoxyoctane were purchased from Aldrich. 7,8-epoxy-2-methoxy-2,6-dimethyloctane (purity 98%) and 1,2-epoxy-1-methylcyclohexane were provided by the DRT company (Castets, France). Water was distilled twice before use.

2.2. Equipments

The stainless steel pressure reactor (50 mL) used for most experiments was one from Parr Instrument Company (maximal pressure (PS) = 200 bar, maximal temperature (TS) = -15 °C– 350 °C, internal diameter (Di) = 3.3 cm, height (h) = 5.5 cm), a magnetic stirring and a heating jacket. The stainless steel pressure reactor (1.2 L) used for the scale-up experiment in DRT (Castets, France) was one from Parr Instrument Company (maximal pressure (PS) = 350 bar, maximal temperature (TS) = 350 °C, internal diameter (Di) = 8.3 cm, height (h) = 24.9 cm), equipped with a heating jacket and a hollow shaft mechanical stirrer.

2.3. Chromatography

Thin layer chromatography (TLC) was performed on silica gel plates Merck 60 F254, and the compounds were visualized by irradiation with UV light or by oxidation with KMnO_4 . Column chro-

matography was carried out using grade silica gel (particle size 0.040–0.063 mm).

2.4. GC-FID analyses

Gas chromatography parameters were adapted depending on the substrate. Products identification was performed by comparison of their retention times with commercial ones. Reaction conversion and selectivity were determined by standard calibration with *n*-dodecane as internal standard. For *Florsantol*[®]: Trace GC Ultra (Thermo Scientific) apparatus with a FID detector was used, equipped with a Thermo Fisher DB-WAX capillary column (30 m, 0.25 i.d., 0.25 f.t.). Parameters were as follows: isotherm temperature was maintained at 135 °C for 22 min, then increased to 160 °C at 2 °C/min and then to 200 °C with a ramp of 30 °C/min (maintained 5 min), injector temperature, 200 °C; detector temperature, 250 °C; injection volume 1 μL , split flow: 50 mL/min, carrier gas (He) 60 kPa. For 1,2-epoxybutane: Analyses were performed on a Shimadzu apparatus with a SH-Trx-Wax column (30 m, 0.25 i.d., 0.25 f.t.). Parameters were as follows: isotherm temperature was maintained at 35 °C for 10 min, then increased from 35 °C to 250 °C at 30 °C/min (maintained 5 min); injector and detector temperature, 250 °C; injection volume 1 μL (split 60:1), carrier gas (He) 60 kPa. For other substrates: The catalytic experiments were followed on Trace GC Ultra (Thermo Scientific) apparatus with a FID detector was used, equipped with a Thermo Fisher HP5-MS capillary column (30 m, 0.25 i.d., 0.5 f.t.) Parameters were as follows: isotherm temperature was maintained at 100 °C for 10 min, then increased to 160 °C at 10 °C/min and then to 220 °C with a ramp of 30 °C/min (maintained 5 min); injector temperature, 200 °C; detector temperature, 250 °C; injection volume 1 μL , split flow: 16 mL/min, carrier gas (He) flow 0.8 mL/min.

2.5. GC-MS analyses

The GC-MS spectra were recorded on a Shimadzu GCMS-QP2010 SE, equipped with an ionization detector (EI) coupled to a simple quadrupole and a Restek SH-RXi-5 ms column (5% diphenyl/95% dimethylpolysiloxane, 30 m \times 0.25 mm \times 0.25 μm). The carrier gas was helium (30 cm/s).

2.6. NMR spectroscopy analyses

^1H and ^{13}C NMR spectra were recorded on a Bruker Avance III 400 MHz spectrometer at 400 MHz for ^1H and 100 MHz for ^{13}C in CDCl_3 with residual CHCl_3 (^1H , 7.26 ppm) or (^{13}C , 77.16 ppm).

2.7. pH measurements

pH values of the suspensions were determined with a Mettler Toledo pH meter without any dilution.

2.8. Zeta potential analyses

Zeta potential measurements were carried out by laser Doppler electrophoresis, with Zetasizer Nano ZS90 equipment. Aqueous suspensions of Pd(0) nanoparticles were diluted at a concentration of $1.9 \times 10^{-3} \text{ mol.L}^{-1}$. Analyses were performed in a cell (DTS1070, 150 μL) at 20 °C. The data was processed by the Zetasizer software.

2.9. Static multiple light scattering – Turbiscan technology

Static multiple light scattering analyses were carried out using the Turbiscan Lab technology (Formulation, Toulouse, France). This apparatus is constituted of a near infrared light source (wavelength $\frac{1}{4}$ 880 nm), and two synchronized detectors, which all move vertically alongside the cylindrical glass sample cell. The light source head scans the entire height of the sample (up to 55 mm), and the detectors acquire transmission and backscattering data every 40 μm . The measured photon fluxes are calibrated with a non-absorbing scattering standard (calibrated polystyrene latex beads) and a transmittance standard (silicon oil). The temperature of the apparatus was regulated at 25.0 ± 0.1 °C. The nanoparticle suspensions were studied without any dilution and for each one of them a scan was carried out every 4 h, along 7 days.

2.10. UV-visible spectroscopy

Measurements were performed in a quartz cuvette with diluted sample, using a Jasco V750 spectrophotometer in the 190–900 nm range (25 °C). The light source was a 340 nm deuterium/halogen lamp.

2.11. TEM experiments

Transmission electron microscopy (TEM) images were recorded with a JEOL TEM 100CXII electron microscope operated at an acceleration voltage of 100 kV, with a KeenView camera and the ITEM software (1376×1032 px). The samples were prepared by the addition of a drop of the colloidal suspension on a copper grid coated with a porous carbon film.

2.11.1. Synthesis of ammonium-stabilized Pd(0) suspension reduced by NaBH_4

The aqueous Pd(0) suspension ($[\text{Pd}] = 3.8 \text{ mmol.L}^{-1}$) was prepared, according to a procedure adapted from the literature [27]. To an aqueous solution (5 mL) of a chosen quaternary ammonium salt ($9.5 \times 10^{-5} \text{ mol}$, 2.5 equiv.) was added 1 mL of a freshly prepared aqueous solution of sodium borohydride ($9.5 \times 10^{-5} \text{ mol}$, 2.5 equiv.). Then, this solution was quickly added under vigorous stirring to an aqueous solution (4 mL) of the sodium tetrachloropalladate(II) hydrate $\text{Na}_2\text{PdCl}_4 \cdot 6\text{H}_2\text{O}$ ($3.8 \times 10^{-5} \text{ mol}$, 1.0 equiv.) to obtain a colloidal suspension of Pd(0). The reduction, indicating by a color change from yellow to black, occurred instantaneously. The suspension was kept under stirring during 12 h before use as catalyst. Zeta potentials of Pd(0) suspensions stabi-

lized by different surfactants were measured and reported in Table S1.

2.12. Synthesis of polyvinylpyrrolidone-stabilized Pd(0) suspension reduced by NaBH_4

To an aqueous solution (5 mL) of PVP (40000 wt) (21 mg, 5 equiv.), was added 1 mL of a freshly-prepared aqueous solution of sodium borohydride ($9.5 \times 10^{-5} \text{ mol}$, 2.5 equiv.). Then, this mixture was quickly added under vigorous stirring to an aqueous solution (4 mL) of the metallic precursor $\text{Na}_2\text{PdCl}_4 \cdot 6\text{H}_2\text{O}$ ($3.8 \times 10^{-5} \text{ mol}$, 1.0 equiv.). A color change from yellow to black was observed, evidencing the reduction. The suspension was kept under stirring for 12 h before use.

2.13. General catalytic procedure

In a 50 mL pressure reactor, 10 mL of Pd(0) suspension (0.038 mmol) and substrate (3.8 mmol) were introduced. In some experiments, additives such as sodium hydroxide or hydrochloric acid could be added to adjust the medium pH to the given value. The autoclave was purged with H_2 (5 bar, 3 times) and pressurized to the given pressure. The reaction mixture was kept at the desired temperature, under magnetic stirring during the desired reaction time. Room temperature refers to 22–25 °C. At the end of the reaction, the products were extracted with diethyl ether ($3 \times 10 \text{ mL}$) and the organic layer was washed with water to remove any trace of acid or base (pH around 7). The crude mixture was analyzed by GC-FID in diethyl ether with *n*-dodecane as internal standard. After purification on column chromatography, the products were analyzed by ^1H and ^{13}C NMR spectroscopy. For the recycling experiment, this aqueous phase was recovered after reaction and a new batch of substrate (3.8 mmol) was introduced in the reaction for another cycle, under same conditions.

2.14. Scale-up for the production of Florsantol[®]

These experiments were carried out using the facilities of the DRT company (Castets, France). In a 1.2 L pressure reactor, the catalyst and 40 g (0.21 mol) of 8-epoxy-2-methoxy-2,6-dimethyl octane (EMDO) were introduced in a molar substrate/Pd ratio of 100. The autoclave was purged with H_2 and pressurized at 40 bar of H_2 . The reactor was heated thanks to a jacket at 85 °C. The reaction was conducted under mechanical stirring with hydrogen circulation thanks to a hollow shaft during 7.2 h. At the end of the reaction, the final products were isolated by solvent extraction (diethyl ether) and analysed by GC-FID.

3. Results and discussion

3.1. Scope of substrates

Pd nanoparticles were synthesized by chemical reduction of sodium tetrachloropalladate (II) with sodium borohydride and efficiently stabilized in water with *N,N*-dimethyl-*N*-cetyl-*N*-(2-hydroxyethyl) chloride (HEA16Cl) in a surfactant/metal molar ratio of 2.5, according to a procedure already reported [27,28]. The Pd@HEA16Cl suspension was investigated for the hydrogenolysis of various epoxides in water (Table 1). According to the substrates, the dihydrogen pressure and the temperature were adapted. In this work, the hydrogenation of epoxystyrene under mild conditions (Table 1, Entry 1) afforded the targeted 2-phenylethanol (75%) as main product, alongside phenylacetaldehyde (12%) and phenylethane-1,2-diol (13%), both formed because of the slightly acidic metal suspension (pH = 5.8). Two alkylphenyl epoxides as

Table 1
Pd(0) nanoparticles-catalyzed hydrogenolysis of various epoxides.^a

Entry	Substrate	Product	T (°C)	PH ₂ (bar)	t (h)	Conversion rate ^b (%)	Selectivity ^b (%)
1			25	1	3.5	> 99	75
2			80	10	4	> 99	90
3			80	10	4	98	94
4			80	10	4	96	100
5			80	10	5	> 99	> 99
6			85	20	17	97	> 99
7			80	30	5	> 99	97 ^c

^a Reaction conditions: Pd (3.8×10^{-5} mol, 0.01 equiv.), HEA16Cl (9.5×10^{-5} mol, 0.025 equiv.), substrate (3.8×10^{-3} mol, 1 equiv.), H₂O (10 mL).

^b Determined by GC. ^c Solvolysis product.

the commercial 2-benzyloxirane and the 2-phenylethoxyirane, synthesized by oxidation of 4-phenylbut-1-ene with *m*-chloroperbenzoic acid, were also evaluated. Distancing the aromatic group from the epoxide function with an alkyl chain (Table 1, Entries 2–3) leads to slower reaction, thus requiring higher conditions (10 bar H₂, 80 °C) to achieve complete conversion in 4 h. The selectivity was driven towards the most substituted alcohol, as observed in the literature owing to electronic effects of the phenyl ring [17–19]. Noteworthy, an inverse selectivity was observed, compared to a quite similar catalyst prepared from the combination of palladium acetate (Pd(OAc)₂) with tetrabutylammonium bromide (*n*Bu₄NBr) [22]. The less reactive aliphatic epoxides (Table 1, Entries 4–6) were reduced after longer reaction times, under harsher conditions (80–85 °C, 10–20 bar H₂), with excellent selectivity (>99%) in the secondary alcohol. This result suggests a steric control of the reaction since the carbon-oxygen bond broken is the one on the less hindered carbon. The hydrogenolysis of cyclic epoxides revealed more challenging, probably due to their rigidity and increased steric hindrance (Table 1, Entry 7). Indeed, even under 30 bar of H₂, the hydrolysis of 1,2-epoxy-1-methylcyclohexane was very fast, leading to the diol exclusively.

Secondly, various capping agents of the particles were evaluated in the hydrogenolysis of epoxystyrene and 7,8-epoxy-2-methoxy-2,6-dimethyloctane EMDO (Tables 2 and 3). The effect of the counter-ion (Cl, H₂PO₄, F) and the polar head length with hydrox-

ybutylammonium (HBA) salt was evaluated and compared to the commercial cetyltrimethylammonium chloride (CTACl). All aqueous suspensions of Pd nanospecies possess positive zeta potential values, superior to + 30 mV, evidencing a good stability due to a significant electrosteric repulsion (Table S1).

3.2. Hydrogenolysis of epoxystyrene.

The hydrogenolysis of epoxystyrene (Table 2) was carried out under mild conditions (1 bar H₂, r.t.) in search of relevant activities and a selectivity into the targeted 2-phenylethanol.

Among the polar heads (Table 2, Entries 1–3), the hydroxyethylammonium (HEA16Cl) salt gave the best kinetics with complete conversion in only 3.5 h, compared to a partial conversion in 4.5 h for the commercial CTACl and HBA16Cl salts. Owing to its lipophilic behavior according to the number of carbon atoms, the surfactant head could influence the size of the micellar organization and the substrate solubility in the aqueous phase, thus modifying the reaction rate. However, with HEA16Cl (Table 2, Entry 1), the diol was observed as co-product, probably owing to the acidic medium (Table S1). Among the counter-ions, fluoride and dihydrogen phosphate gave slower reaction kinetics, compared to the chloride, as already observed with similar catalysts (Table 2, Entries 4–5 vs. 1) [29]. For comparison, the polyvinylpyrrolidone-capped nanocatalyst (Table 2, Entry 6) proved less active with a good

Table 2
Hydrogenolysis of epoxystyrene with Pd-based catalysts.^a

Entry	Catalyst	t (h)	Conversion rate ^b (%)	Selectivity ^b (%)
1	Pd@HEA16Cl	3.5	> 99	75
2	Pd@CTACl	4.5	81	89
3	Pd@HBA16Cl	4.5	63	89
4	Pd@HEA16H ₂ PO ₄	4.5	82	88
5	Pd@HEA16F	4.5	71	87
6	Pd@PVP	3.5	70	93
7	Pd/C (5 wt%)	4.5	> 99	21

^a Reaction conditions: Pd (3.8×10^{-5} mol, 0.01 equiv.), substrate (3.8×10^{-3} mol, 1 equiv.), H₂ (1 bar), room temperature, H₂O (10 mL).

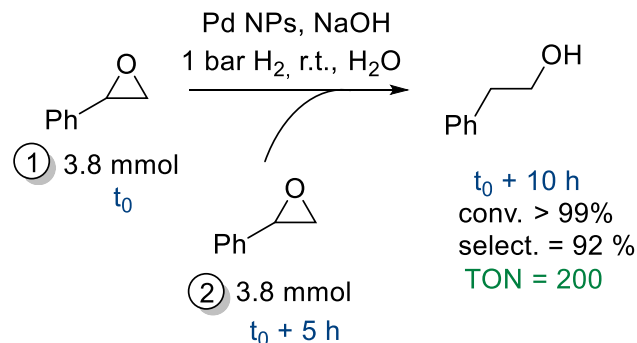
^b Determined by GC.

selectivity in 2-phenylethanol. Similarly, the commercial heterogeneous Pd on charcoal (Table 2, Entry 7) favored the formation of undesired products under similar conditions, mainly the hydrolysis product (71% of diol) and the isomerization one, phenylacetaldehyde (8%), thus proving the efficiency of nanoparticles. Regarding the kinetics, the Pd@HEA16Cl catalyst proves relevant but favors the primary alcohol, alongside with the diol probably formed in the acidic reaction medium. To confirm this hypothesis, the pH of the colloidal suspension was modified by adding hydrochloric acid (pH = 2), leading to the diol predominantly (96% yield) as expected. Thus, to limit the formation of this co-product, the hydrogenolysis reaction was performed in basic conditions with sodium hydroxide (pH = 11), improving the selectivity in primary alcohol up to 92% (Fig. 1). Moreover, the reaction kinetics was also accelerated, with a 76% conversion reached in 3.5 h (compared to 60% at pH = 8). It is noteworthy to underline that without catalyst, the hydrogenolysis of epoxystyrene did not occur in the presence of sodium hydroxide, while in acidic medium the diol was exclusively isolated.

Since phenylacetaldehyde and 1,2-phenylethanediol are potential co-products already reported in the literature [30–32], the formation of 2-phenylethanol starting from these intermediates was checked under reaction conditions. Thus, the reduction of these substrates in the presence of Pd@HEA16Cl was performed, either in standard or basic conditions, but no reaction occurred.

Thus, the Pd@HEA16Cl catalyst proves to selectively open epoxystyrene into 2-phenylethanol in mild and basic conditions with a 84% isolated yield in 5 h, compared to already reported Pd nanoparticles used in water, which require either longer reaction times [22] or higher reaction conditions [19]. Moreover, the catalyst's durability was checked. First, a catalyst's recycling over 4 runs showed a decrease in the catalytic performances (See Fig. S3 in Supporting Information), which could be attributed to a modification of the pH value over the runs from 12 (Run 1) to 5 (Run 4). In the last run, the production of 1-phenylethane-1,2-diol was observed. The addition of NaOH in each run did not improve the selectivity owing to particles aggregation. However, loading the reactor with 3.8 mmol of substrate after this first reaction cycle leads to a complete conversion in 2-phenylethanol after 5 h under the same conditions with no other co-product formed, proving that the catalyst was still active (Scheme 2).

In the literature, the selectivity control in the epoxystyrene hydrogenolysis proved to be tricky with various co-products formed such as 1-phenylethane-1,2-diol [30], phenylacetaldehyde [31,32], acetophenone and oligomers [33] or ethylbenzene [34,35].



Scheme 2. Activity and stability of the catalyst. TON: Turnover Number.

The process developed herein proved to be highly selective in the target rose-smell alcohol with a good Turnover Number of 200.

3.3. Hydrogenolysis of EMDO.

The selective hydrogenolysis of 7,8-epoxy-2-methoxy-2,6-dimethyl octane (EMDO) constitutes a paramount transformation for fragrance industry, affording Florsantol[®], a sandalwood odorant with a flowery and woody note. This less reactive substrate was hydrogenated under higher conditions (20 bar H₂, 85 °C) to achieve a 97% conversion in 17 h (Table 3, Entry 1 vs. 2).

Concerning the polar head (Table 3, Entries 2, 5–6), the CTACl and HEA16Cl salts afforded higher performances than HBA16Cl, with total conversion in 17 h. The chloride salt was the most efficient in term of kinetics, compared to fluoride and hydrogenophosphate ones (Table 3, Entries 2 vs. 7–8). The low conversion (54%) observed with HEA16H₂PO₄ salt could be explained by the suspension destabilization after reaction, attributed to a modification of the counter anion from H₂PO₄⁻ to HPO₄²⁻ (pKa H₂PO₄⁻ / HPO₄²⁻ = 7.2) at the pH measured for the suspension of 6.8 (Table S1). The Pd@PVP particles proved less active than the Pd@HEA16Cl ones, with only 60% conversion in 24 h (Table 3, Entry 9). This slower kinetics could be explained by a strong interaction between the polymer and the lipophilic substrate limiting its access to the metal surface. In all experiments, a selectivity in the secondary alcohol was achieved and the targeted Florsantol[®] was isolated with a 84% yield. However, using Pd/C catalyst in water, a lower selectivity in this odorant (85%) was observed, due to the formation of the primary alcohol (5%) and surprisingly the 7-methoxy-3,7-dimethyloctan-2-ol (11%) through a deoxygenation reaction

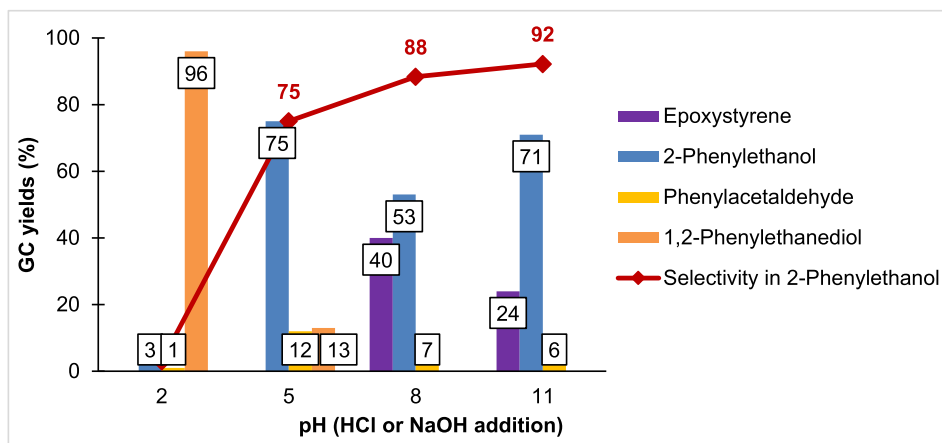
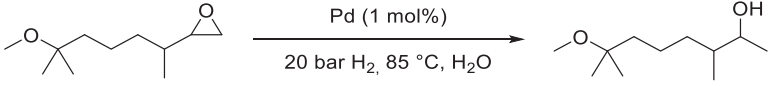


Fig. 1. Influence of the pH in the hydrogenolysis of epoxystyrene. Reaction conditions: Pd (3.8×10^{-5} mol, 0.01 equiv.), styrene oxide (3.8×10^{-3} mol, 1 equiv.), H₂O (10 mL), 1 bar H₂, r.t. 3.5 h. GC yields determined with *n*-dodecane as internal standard.

Table 3
Hydrogenolysis of EMDO with Pd-based catalysts.^a


Entry	Catalyst	t (h)	Conversion rate ^b (%)	Selectivity ^b (%)
1 ^c	Pd@HEA16Cl	17	57	> 99
2	Pd@HEA16Cl	17	99	> 99
3 ^d	Pd@HEA16Cl	24	96	> 99
4 ^e	Pd@HEA16Cl	24	57	100
5	Pd@CTACl	17	99	> 99
6	Pd@HBA16Cl	17	83	98
7	Pd@HEA16H ₂ PO ₄	17	54	98
8	Pd@HEA16F	24	94	> 99
9	Pd@PVP	24	60	99
10	Pd/C (5 wt%)	24	> 99	85

^a Reaction conditions: Pd (3.8×10^{-5} mol, 0.01 equiv.), substrate (3.8×10^{-3} mol, 1 equiv.), 20 bar H₂, 85 °C, H₂O (10 mL).

^b Determined by GC.

^c Reaction performed at 10 bar H₂, r.t.

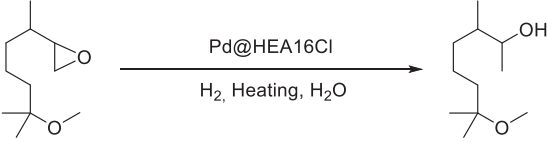
^d Second run in same conditions as Entry 2.

^e Third run in same conditions as Entry 2, Reaction time not optimized.

(Table 3, Entry 10). Moreover, the Pd@HEA16Cl catalyst proved to be reusable through a biphasic approach. A slight decrease in activity was observed but could be restored by extending the reaction time and the excellent selectivity, superior to 99%, was maintained (Table 3, Entry 3). A third run confirmed this tendency, with a decrease in the catalytic activity but an excellent selectivity of 100% (Table 3, Entry 4). Considering these relevant catalytic performances, the hydrogenolysis of EDMO was scaled-up, using the facilities of the DRT company. 40 g of substrate were completely reduced in 7.2 h, at 1 mol% of Pd, under 40 bar H₂ and 85 °C, with a competitive 93% selectivity in the targeted Florsantol[®] of interest for fragrance industry (Table 4, Entry 1). Finally, a scale-up to 175 g of substrate providing a lower metal loading of 0.12% (Entry 2) allowed to achieve a good conversion rate of 87% under a longer reaction time, while maintaining an excellent selectivity of 95%.

3.4. Characterization of the Pd@HEA16Cl catalyst.

The Pd@HEA16Cl, efficient for the targeted reaction, was characterized. First, UV-Vis spectroscopy analyses ($\lambda = 208$ nm) were carried out to follow the reduction kinetics from Pd(II) to Pd(0). The Na₂PdCl₄ solution displayed two absorption peaks around 208.7 nm and 234.0 nm (Fig. S1a), which can be assigned to the charge transfer between the ligand and the metal in the [PdCl₃(H₂O)]⁻ complex [36]. In the Pd@HEA16Cl suspension, the peak at 208.7 nm disappeared and a new one appeared around 225 nm, proving the reduction of Pd (II) to Pd (0) species [37]. The UV absorption of the colloidal suspension was performed over

Table 4
Scale-up of EDMO hydrogenolysis with Pd@HEA16Cl catalyst.^a


Entry	Substrate (g)	Pd loading (%)	Conditions	Conversion rate ^b (%)	Selectivity ^b (%)
1	40	1	40 bar H ₂ , 85 °C, 7.2 h	> 99	93
2	175	0.12	40 bar H ₂ , 100 °C, 25 h	87	95

^a Reaction conditions: [Pd] = 3.8 mM, Substrate, H₂, H₂O.

^b Determined by GC.

time at 208 nm as soon as the reducing agent (NaBH₄) was added to the reaction medium (Fig. S1b). The reduction of palladium was complete after 30 min. The size and morphology of the particles in basic conditions were characterized by Transmission Electron Microscopy and compared to the standard suspension (Fig. 2). In both cases, spherical particles are formed, a slight increase in size (~5.0 nm) was observed in basic conditions, compared to the standard ones (~2.5 nm).

To prove the catalyst's durability, the stability of the aqueous Pd@HEA16Cl suspension was performed with Turbiscan technology that detects phenomena such as sedimentation or creaming (Fig. S2) [38,39]. The transmission and backscattering curves prove that the Pd@HEA16Cl colloidal suspension is stable. Despite a slight increase in the backscattered signal on the bottom of the tube and an increase in the transmitted signal on the top of the tube, the Turbiscan Stability Index (TSI), a statistical parameter that increases with the destabilization of the system, remains inferior to 2 after 7 days. This efficient stabilization could be corroborated with the high potential Zeta value of + 55 mV, measured for the Pd@HEA16Cl suspension (Table S1).

3.5. Mechanistic studies.

Catalytic reductive opening of epoxides by heterogenized Pd species constitutes a strategic way to selectively produce alcohols but its mechanism still remains unclear. The formation of PdH species is usually admitted through the dissociative adsorption of H₂ on the active surface sites of Pd NPs [2,40].

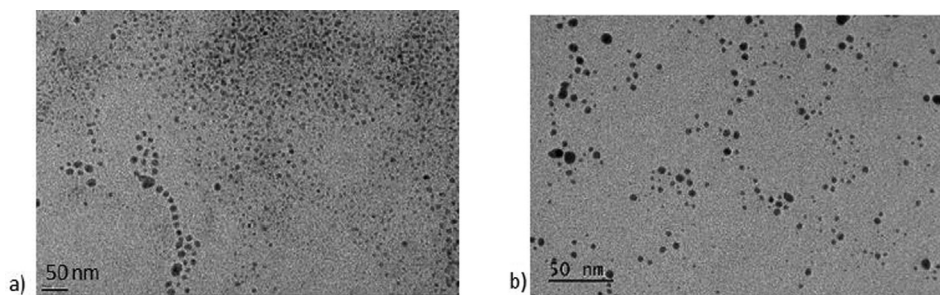
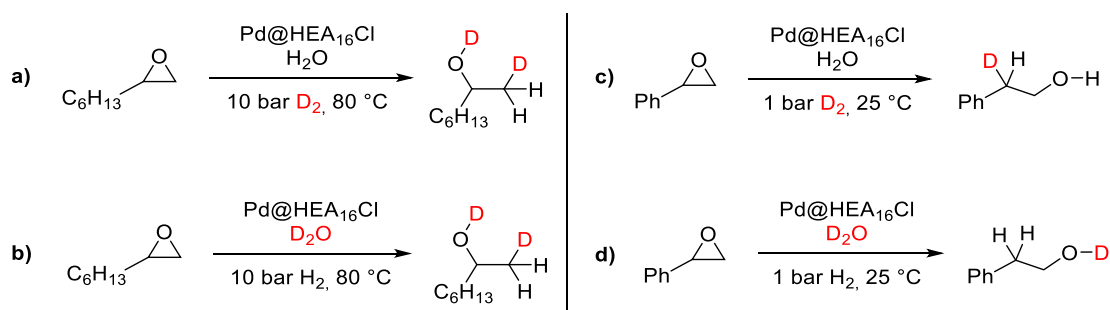


Fig. 2. TEM pictures of the a) standard Pd@HEA16Cl aqueous suspension and b) modified with NaOH up to pH 11.



Scheme 3. Deuterium labelling with D_2 as gas or D_2O as solvent in the reduction of a-b) epoxyoctane and c-d) epoxystyrene.

In this study, deuterium labelling experiments supported with NMR analysis (see ESI for NMR data) were conducted for the reduction of 1,2-epoxyoctane as model substrate of aliphatic epoxides and epoxystyrene, to better understand the different selectivity observed. Epoxyoctane (Scheme 3a) afforded under 10 bar of D_2

at 80 °C the deuterated alcohol on both positions (see Fig. S24). However solvent could not be excluded as a potential hydrogen-donor, since the reaction in D_2O/H_2 gave the same product (Scheme 3b). H/D exchange onto the metal surface has already been reported in previous studies [41–43]. The deuteration of

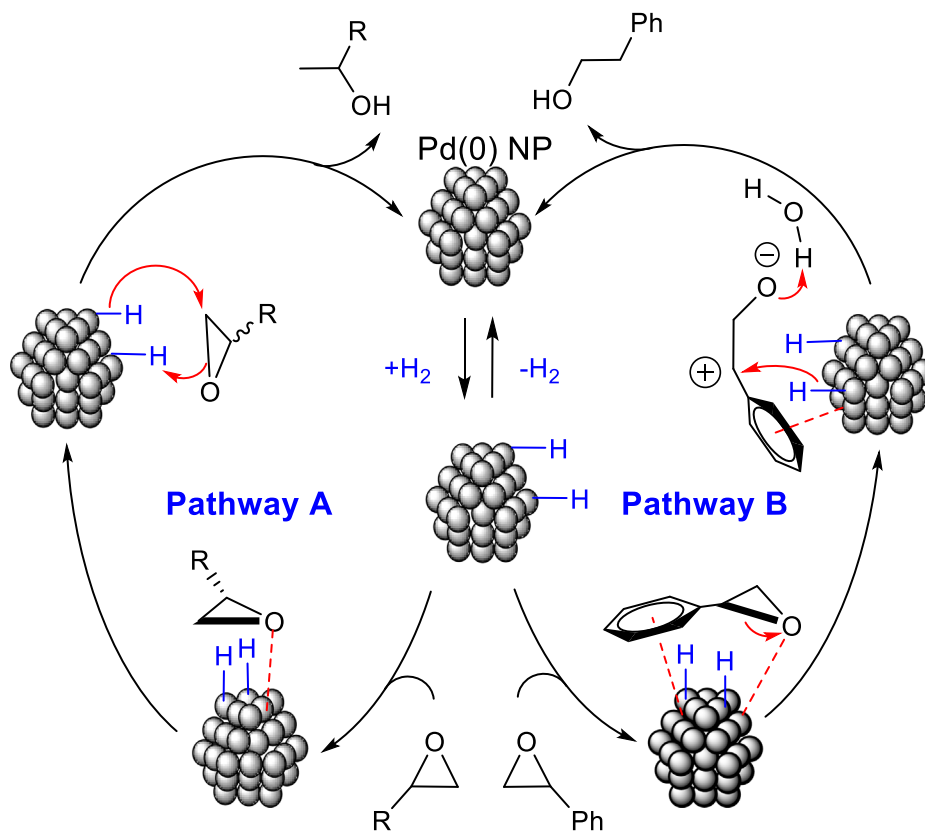


Fig. 3. Proposed mechanism for the Pd nanoparticles hydrogenolysis of terminal epoxides. Steric (Pathway A) vs. Electronic (Pathway B) control.

epoxystyrene at 1 bar D₂ (Scheme 3c) produced the mono-deuterated product (see Fig. S26) and in that case, water seems to act as proton donor. This hypothesis was checked through the hydrogenation of epoxystyrene in D₂O (Scheme 3d), affording the deuterated alcohol (see Fig. S27).

Thus, the mechanism proposed for hydrogenolysis of terminal aliphatic epoxides with Pd nanoparticles using dihydrogen mainly leads to secondary alcohols due to steric hindrance and consecutively the favoured opening (Fig. 3, Pathway A) [44]. The C–O bond could be cleaved thanks to an interaction between the metal and the oxygen atom presumably adsorbed onto the surface by a nearby Pd-bound hydride attack [45].

Concerning epoxystyrene (Fig. 3, Pathway B), the regioselectivity was oriented towards the primary alcohol, as usually observed in the literature [46,12], and could be explained by the strong δ⁺ charge stabilization by the phenyl group in the intermediate, as described by Mitsui [34,44,46]. Moreover, due to the structure rigidity of this aromatic substrate in opposition to a more skeleton flexibility in aliphatic epoxides, a suitable interaction between the π-electrons of the phenyl group and the electrodeficient particle surface could also be mentioned [47,48]. Finally, the metal hydride adds onto the electrodeficient carbon while the alcoholate is immediately protonated in the aqueous reaction medium.

3.6. Conclusions

Aqueous suspensions of hydroxylated ammonium-capped palladium nanoparticles presenting a core size of ca. 2.5 nm proved to be highly efficient for the selective hydrogenolysis of various selected oxiranes, including aromatic, aliphatic, alkylphenyl ones. A thorough study was performed on two target epoxides, epoxystyrene and 7,8-epoxy-2-methoxy-2,6-dimethyloctane (EMDO), whose corresponding alcohols are highly demanded for fragrance industry. In our conditions, the hydrogenation of epoxystyrene proved to be pH-dependent, affording the diol in acidic conditions or the targeted primary alcohol in basic medium. Promisingly, the EDMO was hydrogenated in the industrially targeted Florsantol[®] with a complete selectivity and the catalyst could be recycled after reaction under optimized conditions. A preliminary scale-up up to 40 g of substrate was successfully carried out, showing the potential of the process reported herein as a sustainable alternative to the Vitride process [24] for this sought-after fragrance. A mechanism for the hydrogenolysis of epoxides was proposed, corroborated by deuterium labelling experiments.

Declaration of Competing Interest

The authors declare that they have no known competing financial interests or personal relationships that could have appeared to influence the work reported in this paper.

Acknowledgments

This research project was supported by the ANRT (PhD fellowship). The authors are indebted to Patricia Beaunier from Sorbonne Université (UPMC) for Transmission Electron Microscopy experiments and to the Formulacion company (Toulouse) for the static multiple light scattering analyses conducted in their laboratory with the Turbiscan equipment.

Appendix A. Supplementary data

Supplementary data to this article can be found online at <https://doi.org/10.1016/j.jcat.2021.02.027>.

References

- [1] S. Florio, F.M. Perna, A. Salomone, P. Vitale, Reduction of epoxides, in: P. Knochel, G.A. Molander (Eds.), *Comprehensive Organic Synthesis II*, Elsevier Ltd, 2014, pp. 1086–1122.
- [2] E. Thiery, J. Le Bras, J. Muzart, *Eur. J. Org. Chem.* 2009 (2009) 961–985.
- [3] D.K. Murphy, R.L. Alumbaugh, B. Rickborn, *J. Am. Chem. Soc.* 91 (1969) 2649–2653.
- [4] M. Hudlicky, *Reductions in Organic Chemistry*, second ed., American Chemical Society, Washington, DC, 1996.
- [5] B. Török, T. Dransfield, *Green Chemistry, An inclusive approach*, Elsevier Inc., Amsterdam, The Netherlands, 2018.
- [6] R. Boethling, A. Voutchkova-Kostal, *Green Processes: Designing Safer Chemicals*, Wiley VCH, Weinheim, 2013.
- [7] C. Yao, T. Dahmen, A. Gansäuer, J. Norton, *Science* 364 (2019) 764–767.
- [8] W. Liu, W. Li, A. Spannenberg, K. Junge, M. Beller, *Nat. Catal.* 2 (2019) 523–528.
- [9] S. Thiyagarajan, C. Gunanathan, *Org. Lett.* 21 (2019) 9774–9778.
- [10] M. Ito, M. Hirakawa, A. Osaku, T. Ikariya, *Organometallics* 22 (2003) 4190–4192.
- [11] H. Sajiki, K. Hattori, K. Hirota, *Chem. Commun.* (1999) 1041–1042.
- [12] I. Kirm, F. Medina, X. Rodríguez, Y. Cesteros, P. Salagre, J.E. Sueiras, *J. Mol. Catal. A: Chem.* 239 (2005) 215–221.
- [13] T. Sigeru, O. Hiroshi, N. Seizo, K. Takayuki, *Chem. Lett.* 18 (1989) 1975–1978.
- [14] D. Astruc, *Nanoparticles and Catalysis*, Wiley-VCH, Weinheim, 2008.
- [15] F. Tao, *Metal Nanoparticles for Catalysis: Advances and Applications*, Cambridge, 2014.
- [16] H. Hirakawa, Y. Shiraishi, H. Sakamoto, S. Ichikawa, S. Tanaka, T. Hirai, *Chem. Commun.* 51 (2015) 2294–2297.
- [17] S.V. Ley, C. Mitchell, D. Pears, C. Ramarao, J.-Q. Yu, W. Zhou, *Org. Lett.* 5 (2003) 4665–4668.
- [18] M.S. Kwon, I.S. Park, J.S. Jang, J.S. Lee, J. Park, *Org. Lett.* 9 (2007) 3417–3419.
- [19] S. Nandi, P. Patel, A. Jakhar, N.H. Khan, A.V. Biradar, R.I. Kureshy, H.C. Bajaj, *Chem. Select* 2 (2017) 9911–9919.
- [20] D. Prat, A. Wells, J. Hayler, H. Sneddon, C.R. McElroy, S. Abou-Shehah, *P.J. Dunn, Green Chem.* 18 (2016) 288–296.
- [21] M.-O. Simon, C.-J. Li, *Chem. Soc. Rev.* 41 (2012) 1415–1427.
- [22] E. Thiery, J. Le Bras, J. Muzart, *Green Chem.* 9 (2007) 326–327.
- [23] G.D. Yadav, Y.S. Lawate, *Ind. Eng. Chem. Res.* 52 (2013) 4027–4039.
- [24] R. Parthasarathy, N. Sulochana, *Flavour Frag. J.* 31 (2016) 120–123.
- [25] M.G. Angelo da Silva, M.R. Meneghetti, A. Denicourt-Nowicki, A. Roucoux, *RSC Adv.* 3 (2013) 18292–18295.
- [26] M.G. Angelo da Silva, M.R. Meneghetti, A. Denicourt-Nowicki, A. Roucoux, *RSC Adv.* 4 (2014) 25875–25879.
- [27] B.L. Albuquerque, A. Denicourt-Nowicki, C. Mériadec, J.B. Domingos, A. Roucoux, *J. Catal.* 340 (2016) 144–153.
- [28] B. Léger, A. Nowicki, A. Roucoux, J.-P. Rolland, *J. Mol. Catal. A: Chem.* 266 (2007) 221–225.
- [29] C. Carvalho Rocha, T. Onfroy, J. Pilmé, A. Denicourt-Nowicki, A. Roucoux, F. Launay, *J. Catal.* 333 (2016) 29–39.
- [30] X. Zhu, K. Venkatasubbaiah, M. Weck, C.W. Jones, *J. Mol. Catal. A: Chem.* 329 (2010) 1–6.
- [31] S.M. Islam, P. Mondal, K. Tuhina, A.S. Roy, *Chem. Technol. Biotechnol.* 85 (2010) 999–1010.
- [32] S. Murru, K.M. Nicholas, R.S. Srivastava, *J. Mol. Catal. A: Chem.* 363–364 (2012) 460–464.
- [33] H. Fujitsu, S. Shirahama, E. Matsumura, K. Takeshita, I. Mochida, *J. Org. Chem.* 46 (1981) 2287–2290.
- [34] S. Mitsui, S. Imaizumi, M. Hisashige, Y. Sugi, *Tetrahedron* 29 (1973) 4093–4097.
- [35] R. Ravichandran, S. Divakar, *J. Mol. Catal. A: Chem.* 137 (1999) 31–39.
- [36] Q. Shen, Q. Min, J. Shi, L. Jiang, J.-R. Zhang, W. Hou, J.-J. Zhu, *J. Phys. Chem. C* 113 (2009) 1267–1273.
- [37] S. Tang, S. Vongehr, Z.R. Zheng, X.H. Meng, *Nanotechnology* 23 (2012) 255606.
- [38] O. Mengual, G. Meunier, I. Cayré, K. Puech, P. Snabre, *Talanta* 50 (1999) 445–456.
- [39] S.U. Nandanwar, M. Chakraborty, S. Mukhopadhyay, K.T. Shenoy, *Cryst. Res. Technol.* 46 (2011) 393–399.
- [40] R. Duš, E. Nowicka, Z. Wolfram, *Surface Sci.* 216 (1989) 1–13.
- [41] T. Dwars, G. Oehme, *Adv. Synth. Catal.* 344 (2002) 239–260.
- [42] H.-H. Limbach, T. Pery, N. Rothermel, B. Chaudret, T. Gutmann, G. Buntkowsky, *Phys. Chem. Chem. Phys.* 20 (2018) 10697–10712.
- [43] Y.G. Dai, X. Chu, C. Jiang, Y. Yao, Z. Guo, C. Zhou, C. Wang, H. Wang, Y. Yang, *J. Catal.* 364 (2018) 192–203.
- [44] J. Muzart, *Eur. J. Org. Chem.* (2011) 4717–4741.
- [45] G.C. Accrombessi, P. Geneste, J.-L. Olive, A.A. Pavia, *J. Org. Chem.* 45 (1980) 4139–4143.
- [46] M. Viswanadhan, A. Potdar, A. Divakaran, M. Badiger, C. Rode, *Res. Chem. Intermed.* 42 (2016) 7581–7595.
- [47] M.S. Maung, Y.-S. Shon, *J. Phys. Chem. C* 121 (2017) 20882–20891.
- [48] B. Van Vaerenbergh, J. Lauwaert, P. Vermeir, J. De Clercq, J.W. Thybaut, Chapter One - Synthesis and support interaction effects on the palladium nanoparticle catalyst characteristics, in: C. Song (Ed.), *Advances in Catalysis*, Academic Press, 2019, pp. 1–120.